

FIGURE S1

A

VP882 (cl) MNFGNVIRRLRKAKGWTLQQRVCEEMNGAIQTGH---
Algicola sagamiensis (WP_040439340.1) MQFGHVVRRLRKAKGWTLQRLCDEMNGNIIQTGH---
 MJ1 (ORF237) MHMTLGVVIRRI RHAKQWTLQRTCEEVDFQIQPGH---
 Phage VP58.5 (Gp43) MIEIDIGPVLLKRI RYERGLTLQKLSRLTDDKVLPSN---
 Lambda (cl) MSTKKKPLTQEQLEDARRLKAIY EK K KNE LGLSQE SVADKMGMGQSGV

VP882 ---LSRIERGELTPSVYIARNIARSLGTSLDTMLAEADG-GPLAQQVVP
A. sagamiensis ---LSRIERDDLAPNIFIAHAISASLNISLDHILQFANG-GPLAEAH
 MJ1 ---LSRIERGEGIPSIHFVNIISKALGVSIDATIMEVEGKRPIVKVSTT
 Vibriophage VP58.5 ---LSRIE SAGAGATLKTLLTLANALGTSPSDILREAEAG-GDKVITKP
 Lambda GALFNGIINALNAYNAALLAKILKVSVEEFSPSIIAREIYEMYEA VSMQP

VP882 --DPAQRVVPVLSWVQAGLWTS SPTGVPPELCLDKWV VAPRAKLP PRCYA
A. sagamiensis --DHYLRVPLVSWAEAGYWI E SPSFTLSMEHDCWV LPRDKSIPNCF
 MJ1 --EP I PYLP I VSWVQAGSWTDSPPAADPLSCDDWV IAPK-KLPKNCYA
 Vibriophage VP58.5 --QQVLYVPVLSWVQAGTWT E S PEPADGDYDEWVE APR-GASRKA
 Lambda SLRSEYEYVPVFSHVQAGMFSPELRTFTTKGDAERWVSTTK-KASDSAFW

VP882 LEVRGDSMQAQYG--MSFPEGCYI I VDPNRVPENKSFVVA MQTNAEEA
A. sagamiensis LEVRGDSMQSPYG--VSFPEGS I I F VDPNATPKNKSFVIA IQKDADCA
 MJ1 LRVVGDSTM TAPYG--PSFPDGC I I I VDP TKQPE NKSFVVARQEGSDEA
 Vibriophage VP58.5 LRVQGDSTMQAPIG--KSFPEGCC I V VDP TKQADNRSFVVARLADTGEH
 Lambda LEVEGN SMTAPTGS K P SFPD GML I I V DPE QAVEP GDFC IARLGG-DEF

VP882 TFKQLIIEGADKYLKPLNPQYPLLIKIDQEVITCGVV I DMVCHLANGH
A. sagamiensis SFKQLIIDGSEKYLKPLNPQYPLIKIETEILICGVV FDMVYHLSNQ
 MJ1 TFKQLAIEGGTRYL KPLNPQYPLIQINGDTRFCGVVTF I I S Q I
 Vibriophage VP58.5 TFKQLIIDGPHQY LKPLNPYSYRTI EVNSEVHVCGVV LAWGEGYTVNG I
 Lambda TFKKLIRDSGQVFLQPLNPQYPMI PCNE SCSVVGKVI ASQWPEETF G

B

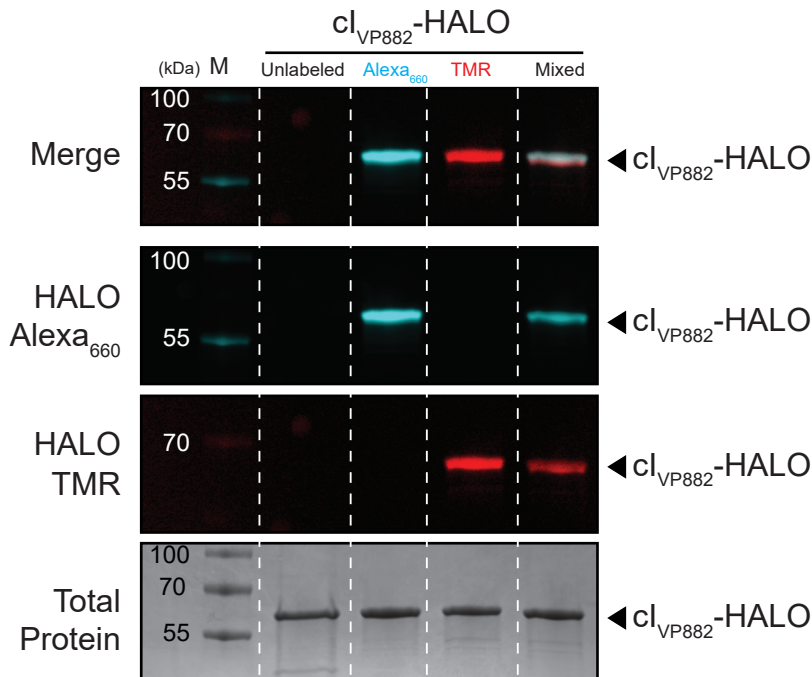


Figure S1. Sequence alignment of cl_{VP882} and other cl -type repressors, and differential HALO-tag labeling to detect proteins by SDS-PAGE analysis, Related to Figures 1, 2, and 3.

(A) Multiple sequence alignment of cl_{VP882} with three related cl -type repressors and cl_{Lambda} . Residues in cl_{VP882} predicted to participate in DNA binding are designated "DNA"; putative catalytic-sites are designated "Catalytic", the cleavage site, between a conserved alanine and glycine residue, is represented with scissors (see Figure 2C), sites in cl_{VP882} and cl_{Lambda} used to fuse domains for chimera construction are represented with crossed-arrows (see Figure 3B), and a site required for Qtip recognition is represented with an asterisk (see Figure 3C). Box shading indicates residues that are identical across all (black), the same in 4 of 5 (dark gray), or in 3 of 5 (light gray) proteins. (B) SDS-PAGE analysis of unlabeled cl_{VP882} -HALO, cl_{VP882} -HALO conjugated to HALO-Alexa₆₆₀ (cyan), cl_{VP882} -HALO conjugated to HALO-TMR (red), or when the separately labeled proteins were combined. Alexa₆₆₀ but not TMR-labeled proteins are detected with the Cy5 filter set, designated HALO-Alexa₆₆₀. TMR- but not Alexa₆₆₀- labeled proteins are detected with the Cy3 filter set, designated HALO-TMR. The composite of the HALO-Alexa₆₆₀ and HALO-TMR channels is shown in the upper-most panel, designated Merge. Unlabeled cl_{VP882} -HALO is not detected using Cy3 or Cy5 filter sets. All proteins can be visualized by staining the gel for total protein with Coomassie Brilliant Blue, designated Total Protein. Molecular weight marker is designated M.

FIGURE S2

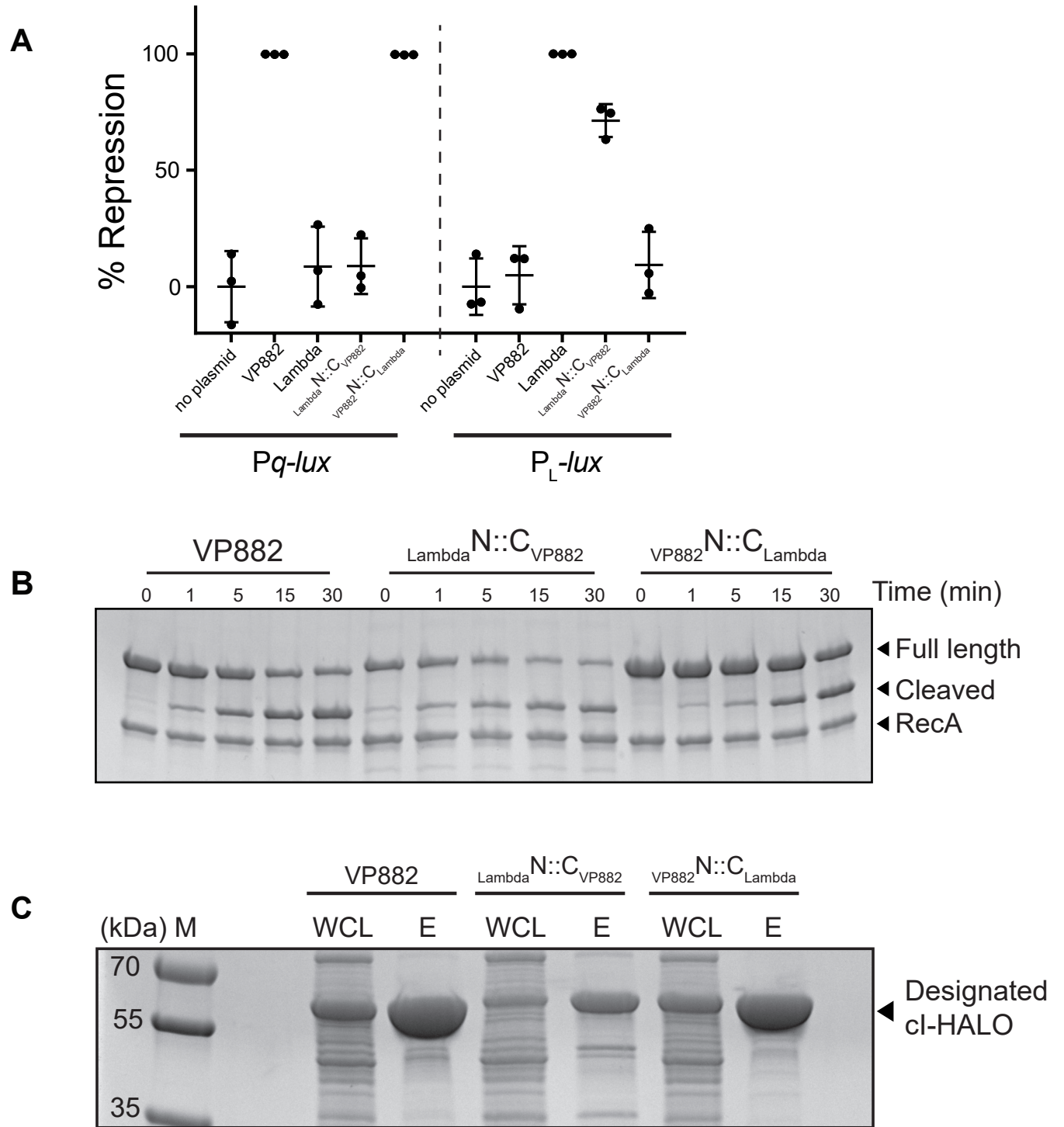


Figure S2. Chimeric *ci* repressors bind DNA and undergo cleavage *in vitro*, Related to Figure 3

(A) Repression of reporter expression by full-length and chimeric *ci* repressors. Left side, percent repression of the VP882-encoded *P_q-lux* reporter or, right side, lambda-encoded *P_L-lux* reporter in *E. coli* lacking (no plasmid) or containing the designated *ci* repressor. %Repression is the difference in RLU obtained for each construct compared to the no-plasmid control. Data represented as mean \pm SD with $n = 3$ biological replicates. (B) *In vitro* cleavage of *ci*_{VP882}-HALO and the chimeric fusions conjugated to HALO-TMR, monitored by SDS-PAGE analysis. Incubation times are noted above each lane. (C) SDS-PAGE analysis of whole-cell lysates (designated WCL) or purified proteins (designated E for eluate) used in (B). Note the lower yield and the presence of possible cleavage products of λ N::C_{VP882}-HALO indicating possible protein instability. Molecular weight marker is designated M.

FIGURE S3

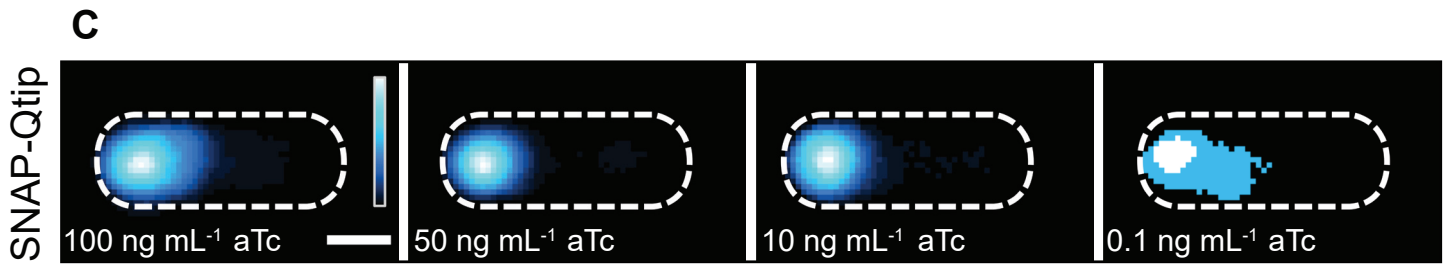
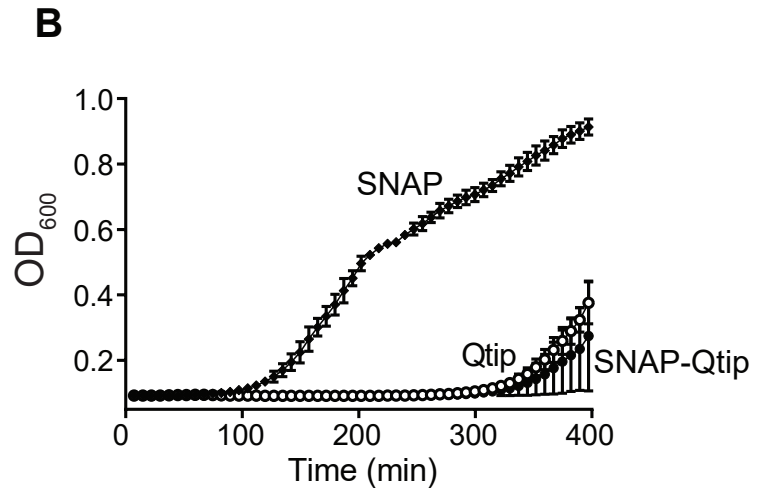
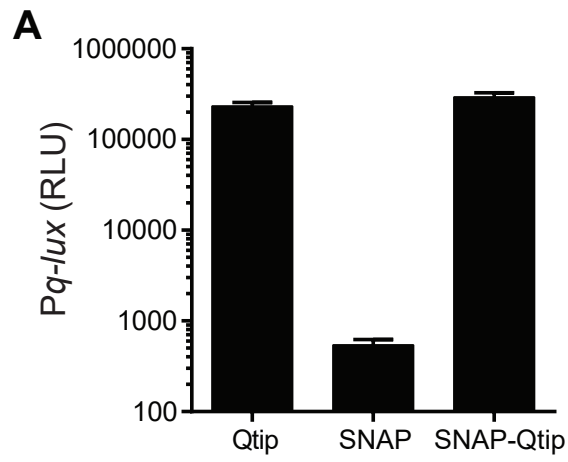


Figure S3. The SNAP tag does not interfere with Qtip function and SNAP-Qtip localizes at the cell poles independent of the concentration of inducer, Related to Figure 4.

(A) Light production from the *P_{q-lux}* reporter in *E. coli* producing *cl_{VP882}* and WT Qtip, SNAP, or SNAP-Qtip. (B) Growth curve of a *Vibrio parahaemolyticus* VP882 lysogen producing the same constructs from (A); SNAP (diamonds), Qtip (open circles), and SNAP-Qtip (closed circles). Data in (A) and (B) represented as mean \pm SD with $n = 3$ biological replicates. (C) Composite images from individual cell analyses of *E. coli* harboring aTc-inducible SNAP-Qtip induced with the indicated amount of aTc. Samples labeled with SNAP-JF₅₀₃ and displayed as in Figure 4A. As noted in the Methods, all images are internally contrasted. The pixelated appearance of the SNAP in the panel showing the 0.1 ng mL⁻¹ aTc concentration is a consequence of low induction of SNAP fluorescence. Scale bar, as in Figure 1D.

FIGURE S4

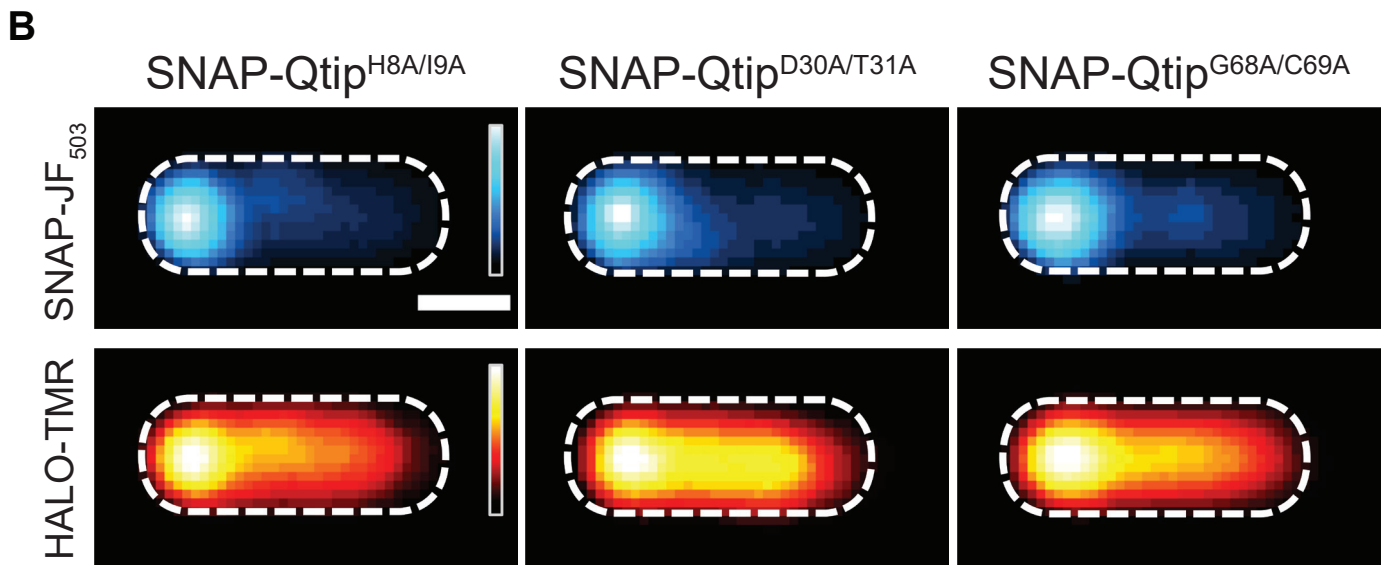
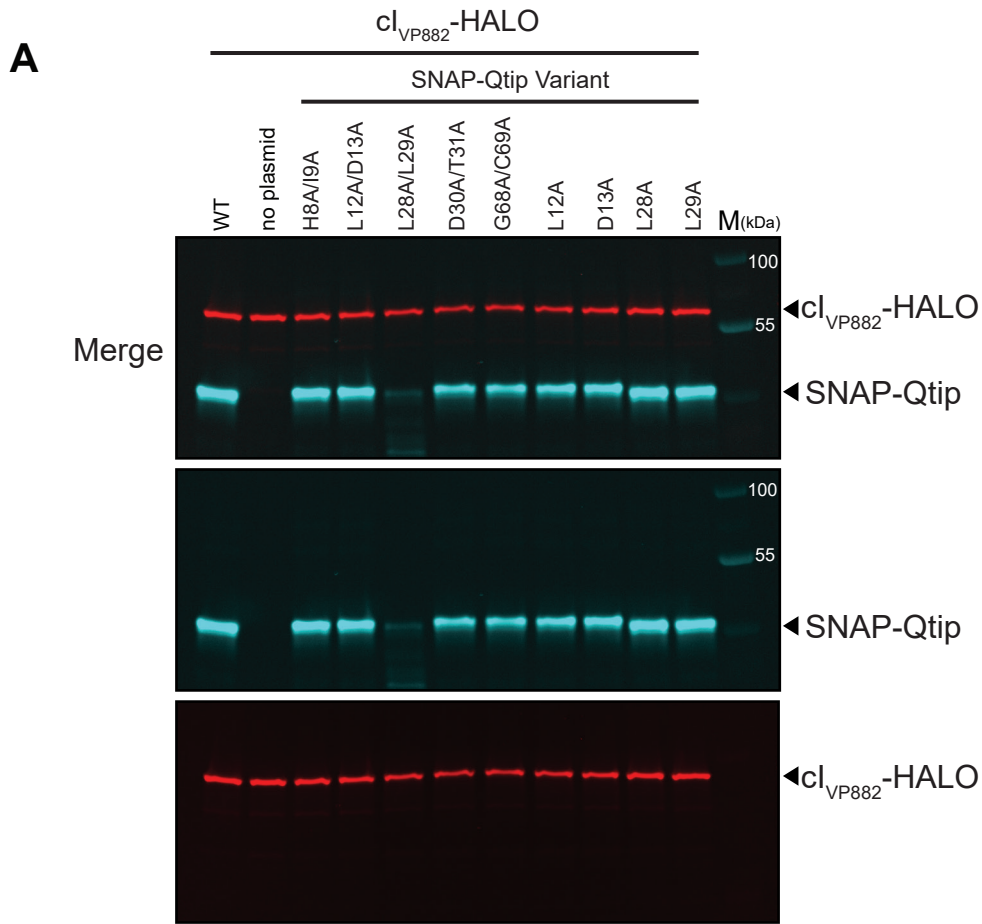


Figure S4. Production of WT SNAP-Qtip and SNAP-Qtip variants, and microscopic analysis of SNAP-Qtip^{H8A/I9A}, SNAP-Qtip^{D30A/T31A}, and SNAP-Qtip^{G68A/C69A}, Related to Figures 4 and 5.

(A) Multi-label SDS-PAGE analysis of *E. coli* harboring one plasmid encoding cl_{VP882}-HALO and either a second plasmid carrying WT SNAP-Qtip (leftmost lane), no plasmid (second lane) or the indicated SNAP-Qtip variant. SNAP-Qtip was labeled with the far-red fluorescent dye SNAP-Cell 647-SiR and cl_{VP882}-HALO was labeled with HALO-TMR. SNAP-Cell 647-SiR (cyan channel) and HALO-TMR (red channel) signals were visualized by imaging the gel under the Cy5 and Cy3 filter sets, respectively, followed by overlaying the channels into a single image (Merge). Molecular weight marker is designated M. (B) Composite images from individual cell analysis of *E. coli* producing cl_{VP882}-HALO and either SNAP-Qtip^{H8A/I9A}, SNAP-Qtip^{D30A/T31A}, or SNAP-Qtip^{G68A/C69A}. Samples labeled with SNAP-JF₅₀₃ and HALO-TMR, and displayed as in Figure 5B. Scale bar, as in Figure 1D.

FIGURE S5

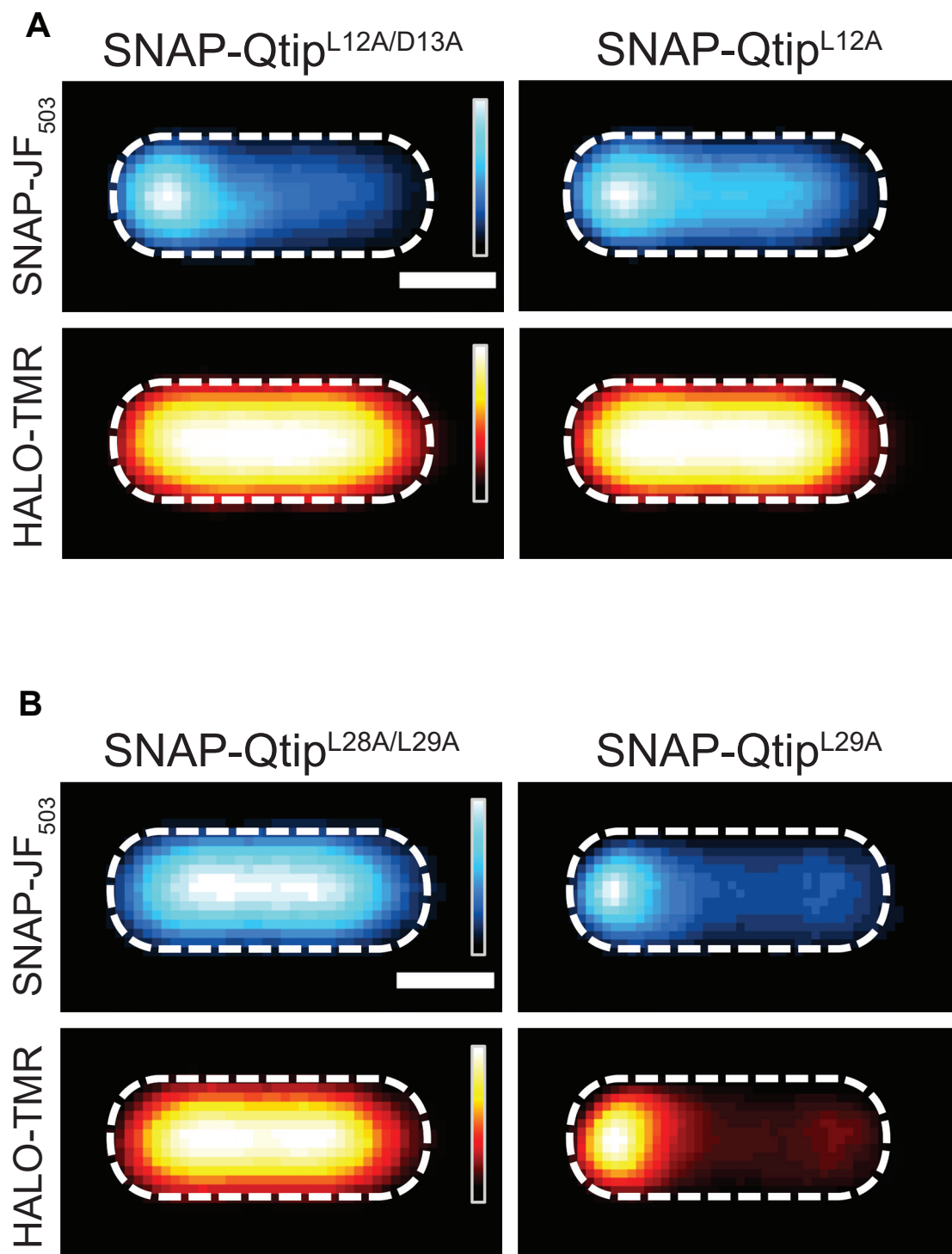
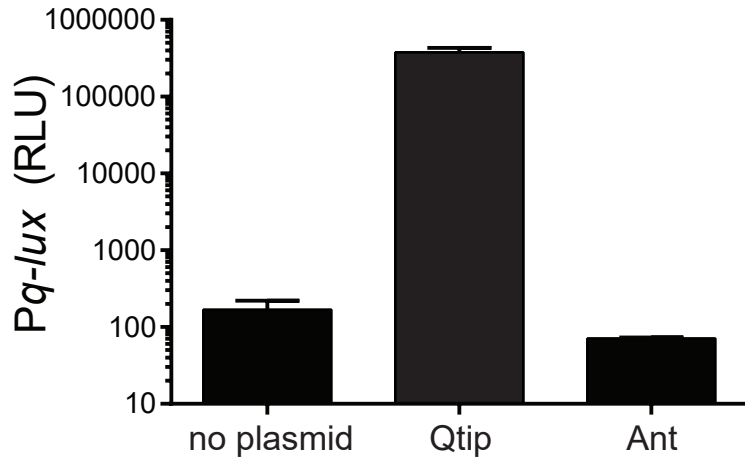


Figure S5. Microscopic analysis of SNAP-Qtip^{L12A/D13A}, SNAP-Qtip^{L12A}, SNAP-Qtip^{L28A/L29A}, SNAP-Qtip^{L29A}, Related to Figures 4 and 5.

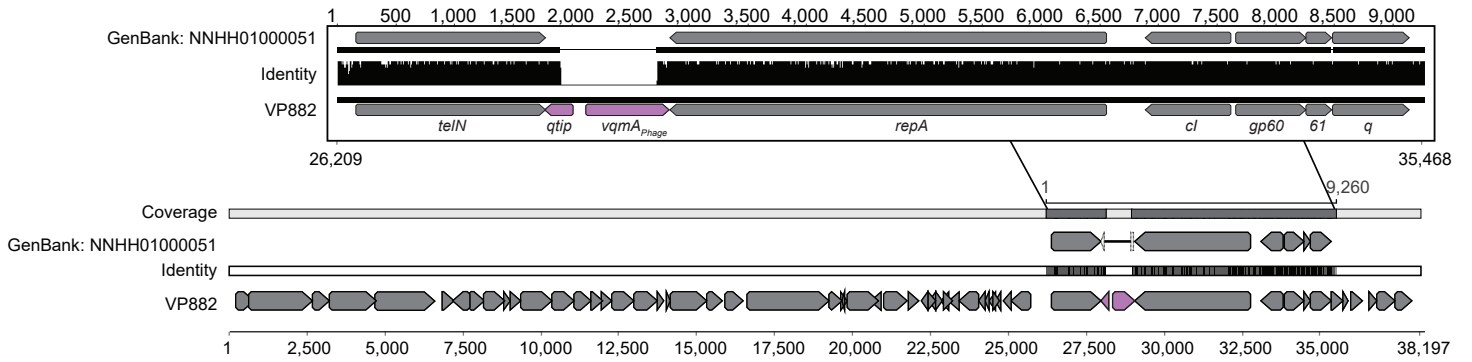
Composite images from individual cell analyses of *E. coli* producing cl_{VP882}-HALO and either SNAP-Qtip^{L12A/D13A}, SNAP-Qtip^{L12A} (A), or SNAP-Qtip^{L28A/L29A}, SNAP-Qtip^{L29A} (B). Samples labeled with SNAP-JF₅₀₃ and HALO-TMR, and displayed as in Figure 5B. Scale bars, as in Figure 1D.

FIGURE S6

A



B



C

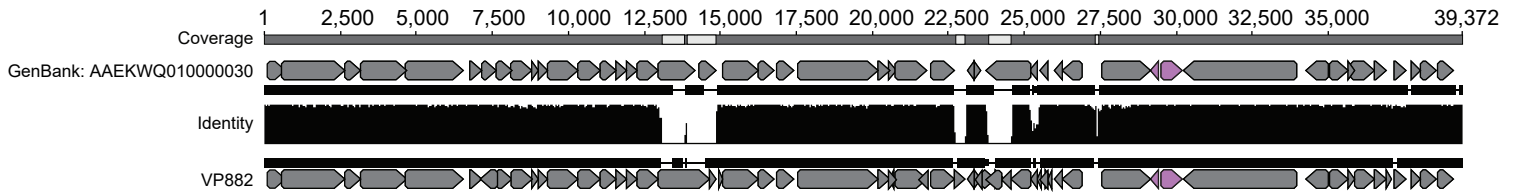


Figure S6. Ant does not induce *Pq-lux* expression, and phage VP882-like elements are present in *Vibrio* and *Salmonella* isolates, Related to Figure 6.

(A) Light production from the *Pq-lux* reporter in *E. coli* producing cl_{VP882} (no plasmid) or cl_{VP882} and a plasmid encoding *Qtip* or *Ant*. RLU as in Figure 1. Data represented as mean \pm SD with $n = 3$ biological replicates. (B) Alignment of GenBank: NNHH01000051 across the VP882 phage genome. Arrows indicate ORFs, purple indicates *qtip* and *vqmA_{Phage}*. Top inset, magnified region of homology across the region containing *qtip* and *vqmA_{Phage}*. Identity plotted between the two alignments with a sliding window size of 1. The gap in the inset indicates the 819 bp deletion in the NNHH01000051 contig. Numbering below and above the alignment indicate the genomic coordinates in phage VP882 and the consensus sequence in the contig, respectively. (C) Alignment of the *Salmonella*-derived element (GenBank: AAEKWQ01000030) across the phage VP882 phage genome. Numbering above the alignment indicates coordinates in the consensus sequence. Identity, gaps, and color scheme as in (B).

Table S1. Bacterial strains used in this study, Related to STAR Methods.

Strain	Genotype	Reference
<i>V. parahaemolyticus</i> O3:K6	Wild-type; phage VP882 lysogen	BCRC 80155
<i>E. coli</i> T7Express lysY/I ^q	<i>E. coli str. B, MiniF lysY lacIq(CamR) / fhuA2 lacZ::T7 gene1 [lon] ompT gal sulA11 R(mcr-73::miniTn10-TetS)2 [dcm] R(zgb-210::Tn10-TetS) endA1 Δ(mcrC-mrr) 114::IS10</i>	NEB
<i>E. coli</i> TOP10	<i>F- mcrA Δ(mrr-hsdRMS-mcrBC) φ80lacZΔM15 ΔlacX74 recA1 araD139 Δ(ara-leu)7697 galU galK λ- rpsL(Str^R) endA1 nupG</i>	Invitrogen
<i>E. coli</i> cl857	<i>E. coli</i> ; λ cl857 lysogen	(Sussman and Jacob, 1962); gift of Tom Silhavy